

The Study of Metal Colloids Produced by Means of Gas Evaporation Technique. I. Preparation Method and Optical Properties in Ethanol

Keisaku KIMURA* and Shunji BANDOW

Instrument Center, Institute for Molecular Science, Myodaiji, Okazaki 444

(Received May 9, 1983)

Three new methods for the preparation of metal colloid in organic solvent are presented. These methods were the matrix isolation method, the gas flow-cold trap method and the gas flow-solution trap method; the latter was found to give a good colloid solution for the optical measurements. The metals reported are high purity Ag, Au, Cu, In, Al, Ca, Sn, and Pb. The stability of the colloid is dependent on the kind of metals: Al, In, Au, and Ag are stable, and Pb, Sn, Ca, and Cu are unstable. The optical absorption spectra of these sols were measured in ethanol solution in Ar atmosphere. They are discussed in relation to those reported on the solid matrix or on the solid substrate.

A considerable amount of literature is available on the optical properties of metal particles in solid matrix as well as in colloidal aqueous solution. The routine methods to make fine particles are that metals are evaporated on an inert substrate and/or rigid matrix in vacuo or that metals are dispersed in an aqueous solution by chemical reaction. The problem posed by the former procedure is the coagulation of particles. In the latter case, we could expect many advances in the study of colloid chemistry, if we can use organic liquids as solvents rather than aqueous solution. The optical spectra were measured at a low temperature for the metal fine particles dispersed on the solid matrix. Except an aqueous solution, there have been very few reports on the spectra of solution state because of the difficulty of the sample preparation.

Conventional chemical methods supply well dispersed particles in a colloid solution; the classical Mie theory¹⁾ has been used to explain the absorption spectrum. Recent measurements of ultrafine particles²⁾ applied both classical and quantum theories to the optical properties of metal particles. However the measurements were limited to solid matrix and to aqueous solution. Therefore it is important for us to observe the spectra of many sorts of metal colloids in organic solvents with a wide range of dielectric constants. Moreover, it will be desirable to get a neat metal colloid solution especially for the study of the physical properties.

In this report, we will present new preparation methods of metal colloids in organic solvents without the use of chemicals such as redox reagents, polymers, electrolytes, glue or other kinds of colloid stabilizers. This method is applied to the measurement of the optical spectra of many metal colloid solutions, some of which are first reported here. The method is applicable not only to ethanol reported here but also to any organic solvent. In addition, this technique can be applied to many sorts of solids as described in this report.

Experimental

Three different preparation methods were examined. These are the matrix isolation method, the gas flow-cold trap method, and the gas flow-solution trap method. All methods are based on a gas evaporation technique.³⁾ The first one is the modification of that described by Wada and Ichikawa.⁴⁾

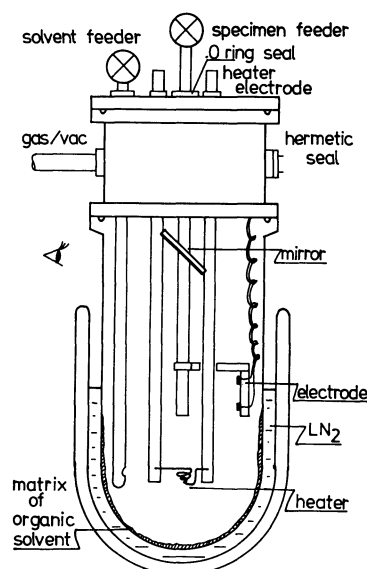
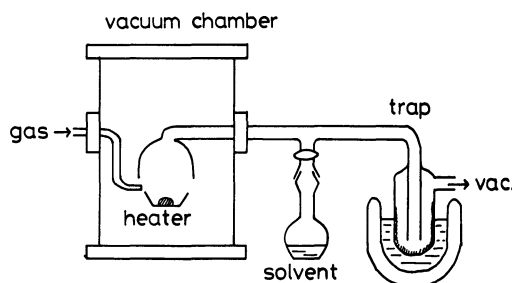


Fig. 1. The apparatus for the matrix isolation method. Organic solvent is introduced through solvent feeder to form matrix on the Pyrex glass dewar which is cooled by liquid nitrogen. Mirror enables us the observation of melting state of metals. Electrode was used to monitor the thickness of the metal layer.

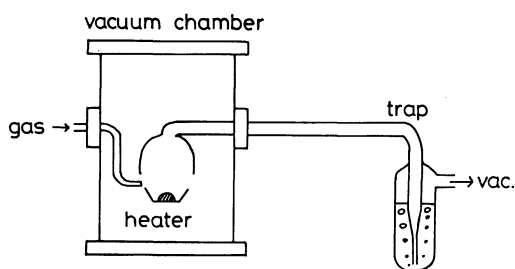


Gas flow - Cold trap

Fig. 2. The apparatus for the gas flow-cold trap method. One of the gas inlet is abbreviated in the Figure.

Therefore we will omit the detailed description of the method and simply show the apparatus used in Fig. 1.

The gas flow-cold trap method is shown in Fig. 2. The fine particles are produced in a vacuum chamber in the atmosphere of helium gas flow. The chamber was once



Gas flow - Solution trap

Fig. 3. The apparatus for the gas flow-solution trap method.

evacuated to 10^{-3} Torr ($1 \text{ Torr} \approx 133.322 \text{ Pa}$) prior to the introduction of helium gas. Under the constant flow of helium gas, a piece of metal was heated. The pressure of the chamber was varied in the range 10–50 Torr corresponding to the desired level of particle diameter. The chamber has two gas inlets, one of which is introduced to the back of tungsten heater to produce fine particles in high efficiency and the other is placed at the edge of the particle collector in order to enhance the collection yield of the particle. Argon was used for this inlet. The vapor of organic solvent which was completely degassed was introduced through the Teflon valve in the carrier gas stream and then trapped in the glass cold trap cooled with liquid nitrogen. After collection of fine particles, the trap was filled with Ar gas at 1 atmospheric pressure. The particle diameter was varied by changing the pressure of gas and the temperature of the heater.

The gas flow-solution trap method is shown in Fig. 3. Two kinds of gases were also used in this case, helium for the production of fine particles and argon for the collection and the carrier of fine particles. The procedure is the same as for the second case, except that the cold trap is replaced by the organic solvent which is cooled by cold ethanol; the temperature is -30 – -40 °C. The matrix isolation method and the gas flow-cold trap method sometimes gave coagulated samples and did not give a finely dispersed solution, on the other hand the gas flow-solution trap method made reproducible, well dispersed solutions. Therefore the results obtained by the latter method are mainly reported in this paper.

All spectra were obtained at room temperature in a conventional fused quartz rectangular optical cell except the vacuum evaporated film on a quartz substrate. The optical absorption spectra were recorded just after the preparation of colloid. Some metals were not stable even under these conditions, as described in the results. The metals reported are silver (99.9999%), gold (99.5%), copper (99.9999%), indium (99.999%), calcium (99.99%), aluminum (99.9999%), lead (99.9999%), and tin (99.9999%). Several organic solvents were tested: ethanol, methanol, tetrahydrofuran, cyclohexane, chlorocyclohexane, cyclohexanone, toluene, and benzene. Some solvents were found to be very reactive toward fine particles and the result of ethanol solution is presented in this report.

The optical absorption spectra of vacuum-evaporated thin films of the metals were also recorded as a reference. The metals were sublimed on the fused silica substrate in a vacuum at least 8×10^{-6} Torr. In the case of calcium, paraffin was sublimed onto the calcium film to prevent the air oxidation during the recording of the spectrum. The film thickness was monitored by a quartz oscillator film thickness gauge, Sloan DTM 200. The electron micrographs were taken by a Hitachi H 500H electron microscope used in the high resolu-

tion mode. The specimen were obtained by dropping the sample solution on the Cu grid coated by collosion film reinforced by carbon film. The silver aqueous colloid was prepared by the conventional chemical method. 0.1 M silver nitrate solution and 1% tannic acid solution were added to 500 ml distilled water and then 1% sodium carbonate solution was poured into the mixture with stirring at 70 °C. The resultant colloid solution was dialysed to distilled water overnight.

Results and Discussion

We examined many organic solvents, as stated in the experimental section, but confine ourselves here to the case of ethanol which has both protic and aliphatic properties.

Pb. Figure 4a shows the micrograph of deposited lead colloid on a carbon film taken by the usual transmission technique. The diameters of many particles lie in the region of 10 nm. Figure 4b shows the optical absorption spectra of lead colloid solution (dark brown) in Ar atmosphere. Two absorption maxima at 400 and 250 nm in a 10 nm thickness evaporated film reflect the spectra of the colloid solution. Three bands: 320 nm shoulder, 250 and 215 nm peaks in colloid was found to be time dependent. The 320 and 250 nm bands decreased with time, while the 215 nm peak increased with time. The 215 nm peak was observed in a less stable metal. It is most likely that this peak comes from the

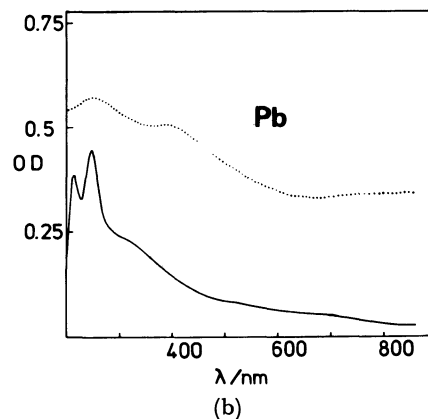
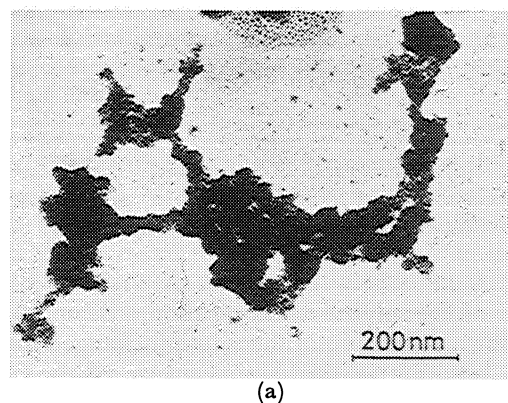
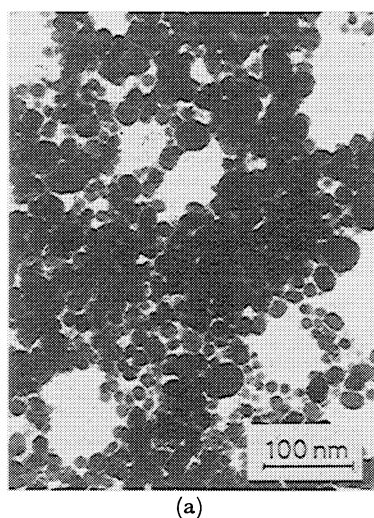
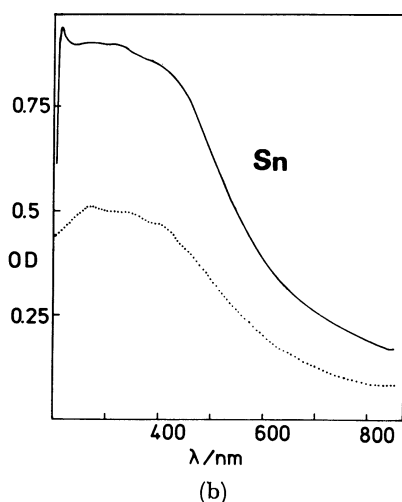


Fig. 4. (a): Micrograph of lead colloid. Small particles aggregate each other to form large particles. (b): Absorption spectra of colloid solution (solid line) and evaporated film (dotted line) of lead. The thickness of the film is 10 nm.



(a)



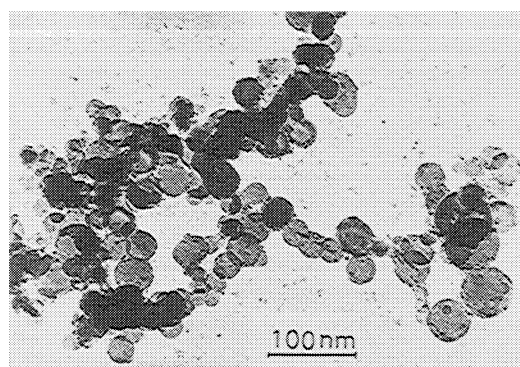
(b)

Fig. 5. (a): Micrograph of tin colloid. (b): Absorption spectra of colloid solution (solid line) and evaporated film (dotted line) of tin. The thickness of the film is 5 nm.

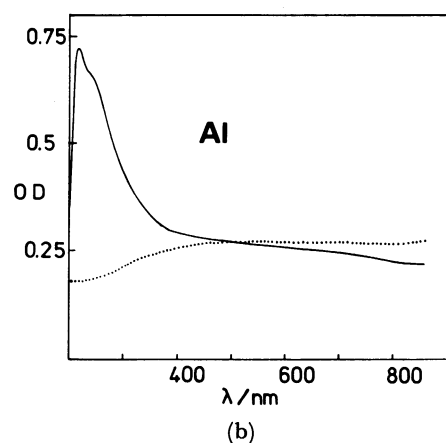
product of the solvent-metal reaction. After 24 h, the dark brown coloration of the solution changed to transparent, resulting in the disappearance of the 320 nm peak.

Lead colloid bands were observed in Pb doped alkali halide crystals. Topa and Velicescu reported⁵⁾ that the colloid band appears at around 250 nm upon annealing the T-center. The computer calculation⁶⁾ on the bases of complete Mie equations agreed fairly well with the above experiment. The peak position depends on the diameter of the particle. Following the calculation, the 240 nm peak was obtained for 10 nm diameter lead colloid-NaCl system. More comprehensive studies were reported by Jain *et al.*⁷⁾ They also observed the Pb colloid band at 240 nm which coincided with the experimental result obtained by Topa and Velicescu. In addition to 240 nm band, they reported that a 214 nm band forms with heat treatment of KCl-Pb system. This band was ascribed to Pb⁰ center. In our case, it is not reasonable to assume the existence of Pb atom in solution to explain the 215 nm peak.

Sn. In Fig. 5a is shown the micrograph of tin colloid. The diameters of many particles fall in the



(a)

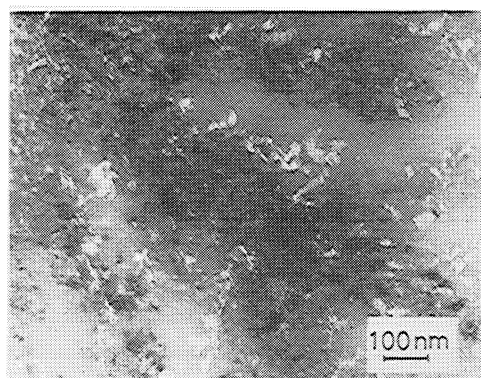


(b)

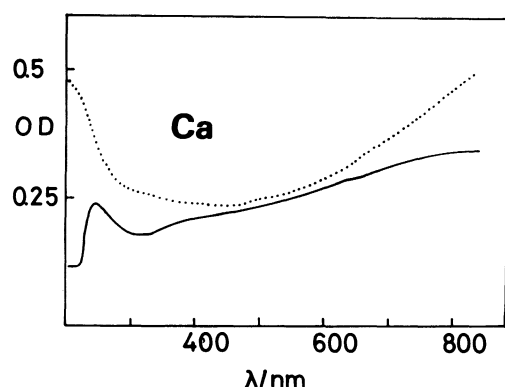
Fig. 6. (a): Micrograph of aluminum colloid. (b): Absorption spectra of colloid solution (solid line) and 20 nm thickness evaporated film (dotted line) of aluminum.

region of 15 nm. Figure 5b shows the spectra of tin colloid solution (dark brown). There is a complex band structure in the region of 240–440 nm of 5 nm thickness evaporated film, which also appears in colloid solution at the same spectral region. We also notice the 215 nm peak due to the solvent-metal reaction. It should be pointed out that the absorption still remains near the infrared region which suggests that the optical properties of this colloid has a bulk nature. The transmission and the reflectance spectra of tin particles isolated by MgF₂ were reported by Zeller and Kuse.⁸⁾ Strong absorption at the visible and near infrared was qualitatively explained by the Maxwell-Garnett theory.⁹⁾ Their result is basically consistent to our data. To complete the identification of the complex absorption band structure, detailed considerations including the surface plasmon and the interband transitions are needed.

Al. In Fig. 6a is shown the micrograph of aluminum colloid. The diameter of the majority is near 30 nm. Figure 6b shows the spectra of aluminum colloid solution (dark blue) together with that of 20 nm thickness evaporated film. Rather strong absorption exists even at 850 nm, although some may be due to scattering effects. There are two peaks at 215 and 250 nm, together with a broad band at around 550 nm. The solution was stable for one month, irrespective of the existence of the 215 nm peak. We assume this stability to be due to the formation of the passive state on the surface of the colloid. The calculation of the optical spectra based on



(a)

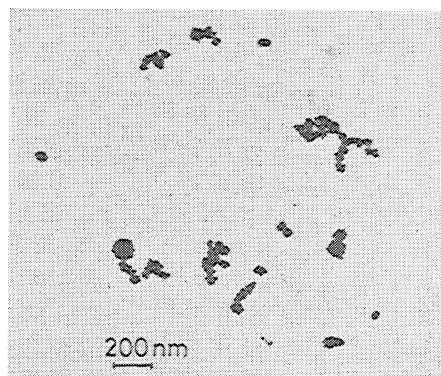


(b)

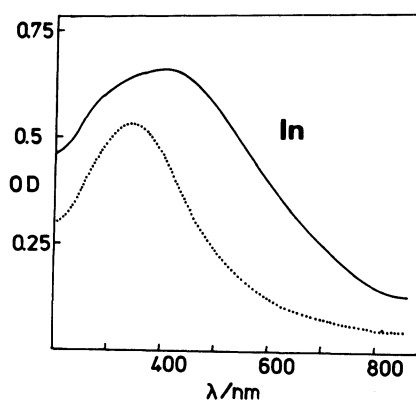
Fig. 7. (a): Micrograph of calcium colloid. Many particles were decomposed during the sample preparation for the measurement of electron microscopy. (b): Absorption spectra of colloid solution (solid line) and 35 nm thickness evaporated film (dotted line) of calcium.

Mie's treatment was conducted for the system of $\text{Al}-\text{Al}_2\text{O}_3$.¹⁰⁾ The 250 nm absorption maximum was obtained for the particles of 10 nm and the 305 nm maximum for 20 nm diameter ones. The difference between the present study and their calculation may lie in the difference of dielectric constant. The spectrum of aluminum aqueous colloid solution prepared by the aerosol technique was reported by Petrov.¹¹⁾ Only a broad band at 600 nm was observed in his study.

Ca. In Fig. 7a is shown the micrograph of calcium colloid. It is difficult to perceive any individual particles in the figure except traces. Figure 7b shows the spectra of calcium colloid solution (light blue) and the 35 nm thickness evaporated film. Calcium was not stable toward oxygen and water, therefore the evaporated film was coated with paraffin and then we measured the spectra. Even upon this treatment, the absorption decreased with time within ten to twenty minutes. The colloid solution was also unstable. The coloration changed to transparent within one hour in the Ar atmosphere, which indicates that the metal particle reacts with the alcohol. The formation of calcium colloid in CaF_2 crystal was reported by Orera and Alcará.¹²⁾ The absorption band at 550 nm in heavily electron irradiated samples and in additively colored crystals of CaF_2 is associated with colloidal calcium. These authors also calculated the optical absorption spectra using Mie's theory and obtained a good agreement between



(a)

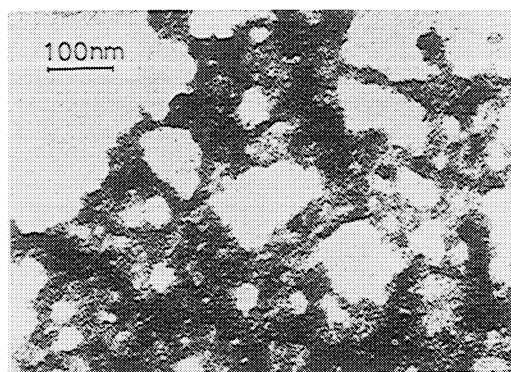


(b)

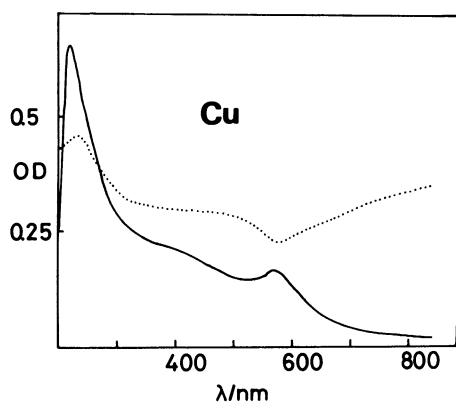
Fig. 8. (a): Micrograph of indium colloid. (b): Absorption spectra of colloid solution (solid line) and evaporated film (dotted line) of indium. The thickness of the film is 5 nm.

theoretical calculations and experimental results.¹³⁾ On the other hand, McLaughlan and Evans observed many bands between 300 and 700 nm on the X-irradiated doped CaF_2 crystal.¹⁴⁾ In the thin film, as shown by Fig. 7b, we have an absorption window in this region. In solution, the absorption minimum shifts to 320 nm and a new peak appears at around 250 nm. We notice that there are many bands between 350 and 850 nm, although they are obscured by the broad distribution of the size of the calcium colloid. The dielectric constant of the solvent and the diameter of the colloid is the main cause of the difference in the solution state and in the rigid matrix.

In. In Fig. 8a is shown the micrograph of indium colloid. The diameters of many particles are scattered from 10 nm to 80 nm. Figure 8b is the absorption spectra of indium colloid (light brown) and the evaporated film whose thickness is 5 nm. The colloid solution was very stable over several months. The optical absorption of indium granular deposits was reported for three samples with different thicknesses on the quartz substrate.¹⁵⁾ The position of the absorption maximum was nearly constant at 258 nm, irrespective of the differences in thickness: 3.5, 7, and 22 nm. The 258 nm peak shifts to 340 nm for the case of thin film (Fig. 8b). In solution, the absorption band seems to be comprised of two peaks: 280 and 400 nm maximum. The reason of this broad band is attributable to the wide diameter distri-



(a)

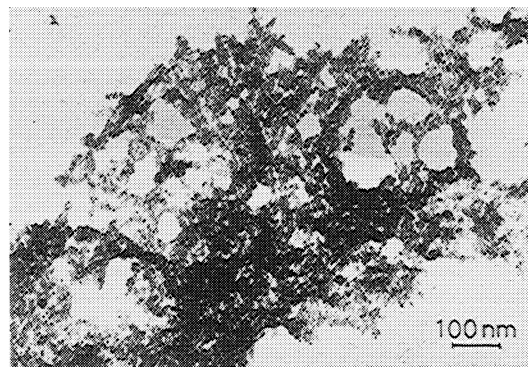


(b)

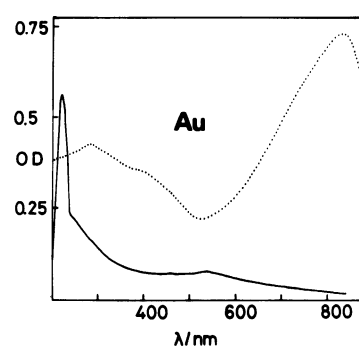
Fig. 9. (a): Micrograph of copper colloid. Very small particles are scattered over the film. (b): Absorption spectra of colloid solution (solid line) and evaporated film (dotted line) of copper. The thickness of the film is 10 nm.

bution in the sols.

Cu. Figure 9a shows the micrograph of copper colloid. The diameter of the majority is near 5 nm. The optical absorption spectra of copper colloid (wine red) and the evaporated film are shown in Fig. 9b. There are two peaks at 220 and 570 nm and two shoulders at 240 and 380 nm. This colloid was not stable in an aerobic condition. The 570 nm peak disappeared within 30 min and the wine red color also disappeared. The 240 nm shoulder slightly increased in intensity at the same time. On the other hand, the colloid was relatively stable under the Ar atmosphere. However, the wine red color changed to yellow after one day. The spectrum of copper colloidal particles was measured in dodecane.¹⁶⁾ Three peaks at 220, 310, and 590 nm were observed. These observations resemble our spectrum closely. The 570 nm peak of copper fine particle was also observed by Abe *et al.* on the Ar matrix at liquid helium temperature.¹⁷⁾ It is noticeable that the room temperature colloid solution gives the same spectrum as that of the fine particles dispersed on low temperature matrices. The optical spectrum of the suspension of copper particles in water was measured by Petrov.¹¹⁾ The two peaks observed at 380 and 590 nm may correspond to 380 and 570 nm peaks in the present study. The origin of the long wavelength peak (570 nm) is not clear: it could be assigned to an interband transition¹⁷⁾



(a)



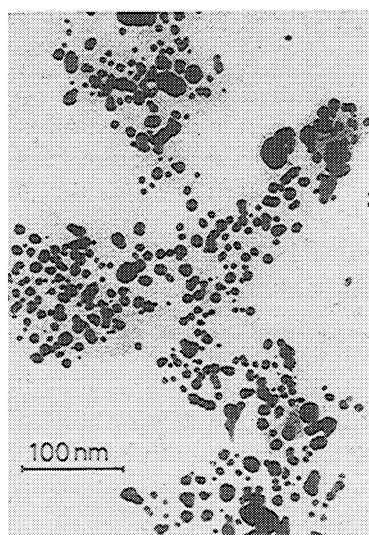
(b)

Fig. 10. (a): Micrograph of gold colloid. Very small particles are scattered over the film. (b): Absorption spectra of colloid solution (solid line) and 10 nm thickness evaporated film (dotted line) of gold.

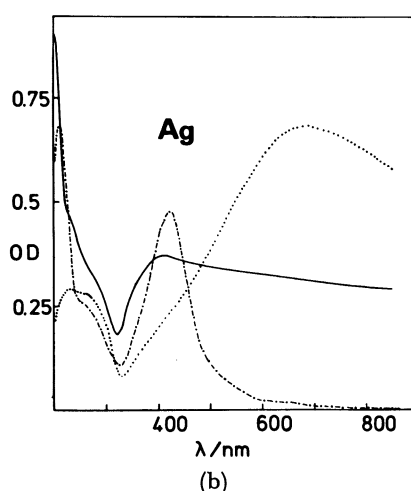
or to an intraband transition.^{11,16)}

Au. In Fig. 10a is shown the micrograph of gold colloid. The diameters of many particles fall in the region from 10 nm to 5 nm. The optical absorption spectra of gold colloid solution (purple) is shown in Fig. 10b, together with that of the evaporated film whose thickness is 10 nm. This colloid is very stable over a month. The absorption spectra of aqueous gold sols and small particles deposited in glass were reported by Doremus.¹⁸⁾ In aqueous gold sols, there are two main peaks at 250 and 520 nm. The 520 nm peak was also found in the deposited particles (12 nm diameter) in glass. In ethanol gold sols, we found three peaks at 220, 250, and 540 nm. Generally speaking, these two sols are quite similar in their spectra, as was the case for the copper colloid, regardless of the difference in solvent and measurement temperature. Abe *et al.*¹⁷⁾ also measured the spectra of gold fine particles in Ar matrix at liquid helium temperature. There were two peaks at 520 and 380 nm. They assigned the 520 nm peak to surface plasmon absorption. Here, we will point again that the gas flow-solution trap method gives a simple and well dispersed particle system, similar to the result of the low temperature Ar matrix method.

Ag. The spectra of silver colloid are given in Fig. 11. For all three samples, the vacuum evaporated film (8.5 nm in thickness), ethanol sols (12 nm in diameter) and aqueous sols (6.4 nm in diameter), there are clear plasmon edges at 330 nm. Absorption peaks are different for three samples (the plasmon peaks are



(a)



(b)

Fig. 11. (a): Micrograph of silver colloid. The diameter of many particles is near 10 nm. What determined by X-ray diffraction is 12 nm. (b): Absorption spectra of ethanol colloid solution (solid line), aqueous colloid solution (broken-dotted line) and 8.5 nm thickness evaporated film (dotted line).

at 420 nm to aqueous sol, at 405 nm to alcohol sol and at 680 nm to thin film) but the general feature is similar for the two sols. There are many reports on the optical properties of silver colloids. Doremus measured¹⁹⁾ the optical absorption spectra of silver particles in glass (the peak at 440 nm) and got a successful agreement with the calculation done using Mie's equation. Genzel *et al.* calculated the plasmon peak and halfwidth of the plasmon peak as a function of particle diameter based on a quantum mechanical model.²⁰⁾ The peak position thus obtained is 407 nm for 10 nm particles. A gas evaporation technique was applied to the measurement of optical absorption of silver microcrystallites at low temperature.¹⁾ The plasmon peak at 380 nm was explained by a classical model. The additional peaks at about 300–340 nm were ascribed to the Ag atom trapped in the matrix in low temperature. The absorption at the ultraviolet region observed in the silver colloid of

the present report may be the contribution from the interband transitions.

Conclusion

A new colloid preparation method, the gas flow-solution trap method, was presented and described in detail. The presented method has three characteristics. One is the wide applicability to any metals/metal solid solutions with use of the same apparatus. It should be emphasized that this technique is not confined to metals but is applicable also to any thermally stable solid samples. The second is the simpleness of the system. This technique gives substantially a two-component pure system unless the metal does not react with solvent. The simpleness of the system may make it easy to understand the solid state properties of small metal particles in solution. The third one is that the colloid prepared by the present method is a sol, that is, the metal fine particles are in solution. This is a merit for the optical measurement in ultraviolet region, because the scattering effect is dominant in solid matrixes in this region.

This technique was applied to Pb, Sn, Al, Ca, In, Cu, Au, and Ag metal colloids in ethanol solution. All metals gave well-dispersed colloids. The diameters of many samples fell in the region of 10 to 50 nm in the present experimental conditions. Some metal particles, Pb, Sn, Ca, and Cu were found to be unstable and others, Al, In, Au, and Ag, were stable. The optical spectra of these colloid solutions resembled the reported spectra of fine particles on matrix or on substrate, many of which were results of low temperature measurements.

References

- 1) G. Mie, *Ann. Phys.*, **25**, 377 (1908).
- 2) H. Abe, W. Schulze, and B. Tesche, *Chem. Phys.*, **47**, 95 (1980).
- 3) S. Yatsuya, S. Kasukabe, and R. Uyeda, *Jpn. J. Appl. Phys.*, **12**, 1675 (1973).
- 4) N. Wada and M. Ichikawa, *Jpn. J. Appl. Phys.*, **15**, 755 (1976).
- 5) V. Topa and B. Velicescu, *Phys. Status Solidi*, **33**, K29 (1969).
- 6) I. S. Radchenko and P. P. Safonenko, *Sov. Phys. Solid State*, **13**, 3132 (1972).
- 7) S. C. Jain, S. Radhakrishna, and K. S. K. Sai, *J. Phys. Soc. Jpn.*, **27**, 1179 (1969); S. C. Jain and K. S. K. Sai, *ibid.*, **30**, 1760 (1971).
- 8) H. R. Zeller and D. Kuse, *J. Appl. Phys.*, **44**, 2763 (1973).
- 9) J. C. Maxwell-Garnett, *Philos. Trans. R. Soc. London*, **205**, 237 (1906).
- 10) I. S. Radchenko, *Sov. Phys. Solid State*, **12**, 2635 (1971).
- 11) Yu. I. Petrov, *Opt. Spectrosc. (U. S. A.)*, **27**, 359 (1969).
- 12) V. M. Orera and R. Alcalá, *Phys. Status Solidi A*, **38**, 621 (1976); *J. Phys. (Paris)*, Colloq. **C7**, 520 (1976).
- 13) V. M. Orera and E. Alcalá, *Phys. Status Solidi A*, **44**, 717 (1977).
- 14) S. D. McLaughlan and H. W. Evans, *Phys. Status Solidi*, **27**, 695 (1968).
- 15) G. Rasigni, J. P. Pètrakian, M. Rasigni, and J. P. Palmari, *J. Phys. C*, **9**, L325 (1976).
- 16) M. Moskovits and J. E. Hulse, *J. Chem. Phys.*, **67**, 4271

(1977).

- 17) H. Abe, K.-P. Charlé, B. Tesche, and W. Schulze, *Chem. Phys.*, **68**, 137 (1982).
- 18) R. H. Doremus, *J. Chem. Phys.*, **40**, 2389 (1964).
- 19) R. H. Doremus, *J. Chem. Phys.*, **42**, 414 (1965).
- 20) L. Genzel, T. P. Martin, and U. Kreibig, *Z. Phys., B*, **21**, 339 (1975).
-